Fuel 111 (2013) 120–130

Contents lists available at SciVerse ScienceDirect

Fuel

journal homepage: www.elsevier.com/locate/fuel

An improved methodology for determining threshold sooting indices from smoke point lamps

Roger J. Watson [a], Maria L. Botero [a], Christopher J. Ness [a], Neal M. Morgan [b], Markus Kraft [a,*]

[a] University of Cambridge, Chemical Engineering & Biotechnology, New Museums Site, Pembroke Street, Cambridge CB2 3RA, United Kingdom
[b] Shell Global Solutions, Shell Technology Centre Thornton, Pool Lane, Ince CH2 4NU, United Kingdom

HIGHLIGHTS

- We examine ways to reduce error in the measurement of threshold sooting index TSI.
- Image analysis is used to determine the height of the flame, an intensity threshold is applied.
- Fuel uptake rate at incipient smoke trail formation is best metric.
- Confidence intervals as low as 1% are obtainable for some fuels.

ARTICLE INFO

Article history:
Received 22 February 2013
Received in revised form 9 April 2013
Accepted 11 April 2013
Available online 28 April 2013

Keywords:
Smoke point
Sooting tendency
Laminar diffusion flame
Intensity image

ABSTRACT

The ASTM D1322 smoke point test has been used for many years as a quick, convenient and easy way to characterize the sooting propensity of aviation fuels. Attempts to apply the same procedure to hydrocarbons in general have been less successful, since for highly sooting fuels the low smoke point makes it very difficult to obtain values with adequate reproducibility. This work describes an adapted version of the test which is usually much more reproducible than the ASTM method, particularly in the case of highly sooting fuels; typically halving the experimental error. The only additional equipment required is an analytical balance of 0.1 mg precision and a PC, together with some modifications to the ASTM D1322 burner which can be carried out in most engineering workshops. The alternative test is based on the fuel uptake rate and image analysis, rather than the height of the flame. An inflexion point is observed when plotting the flame height against fuel uptake rate and is suggested as a reference point to calculate the threshold sooting index (TSI). Results show an improvement in the reproducibility of the observations and a decrease in the error associated with the TSI calculation.

© 2013 Elsevier Ltd. All rights reserved.

1. Introduction

Airborne particulate matter is known to adversely affect human health in many ways; causing harm to the lungs, heart, bloodstream, cardiovascular system and brain [1]. A significant source of this particulate matter is soot generated from internal combustion engines. In order to assess the environmental impact of a given fuel blend, there are two major requirements:

1. An objective measure of the overall sooting propensity of the fuel blend.
2. Information about the particle size distribution (PSD), as particles of diameter below 100 nm are significantly more harmful than larger particles, as well as remaining airborne for much longer [2].

Ultimately, a predictive model to describe both the sooting propensity and the PSD is required, and some progress has already been made towards this goal [3–8], however experimental data are required to aid model development. This work will focus on the simpler problem of how to quantify sooting propensity based on robust and reproducible measurements.

A widely used metric for the sooting propensity of a fuel is the ASTM D1322 smoke point test; particularly in the case of aviation fuels. The test uses a standardized apparatus involving a wick-fed laminar diffusion flame to quantify sooting propensity in terms of the height of the flame for incipient production of visible soot. This height is known as the smoke point. According to the ASTM standard, the process of obtaining the smoke point requires that the flame be progressed through the following stages:

1. A long tip; smoke slightly visible; erratic and jumpy flame.
2. An elongated, pointed tip with the sides of the tip appearing concave upward as shown in Fig. 1a (Flame A).

* Corresponding author.
E-mail address: mk306@cam.ac.uk (M. Kraft).

0016-2361/$ - see front matter © 2013 Elsevier Ltd. All rights reserved.
http://dx.doi.org/10.1016/j.fuel.2013.04.024

Nomenclature

Lower-case roman

M_W	molecular weight of fuel (g mol^{-1})
h	smoke point (mm)
a, b	apparatus-dependent constants (variable units)
N_P	length of the video image of the flame (pixels)
H_{real}	actual flame height (mm)
H_{rod}	height of the video image of the calibration rod (mm)
H_{vid}	overall height of the video image (mm)

Lower-case greek

θ	equivalence ratio, dimensionless
σ	error, various dimensions

Subscripts

1	value for the reference fuel with the higher TSI
2	value for the reference fuel with the lower TSI
h	constants determined based on smoke point measurements
e	constants determined based on critical equivalence ratio
V	constants determined based on volumetric flow rate of fuel
pure	refers to pure fuel
blend	refers to blended fuel

Abbreviations

TSI	Threshold Sooting Index
YSI	Yield Sooting Index
MPI	Micropyrolysis Index
O&P	method of Olson et al. [10]

3. The pointed tip just disappears, leaving a very slightly blunted flame as shown in Fig. 1a (Flame B). Jagged, erratic, luminous flames are sometimes observed near the true flame tip; these shall be disregarded.

The height of the flame at point B is recorded to the nearest 0.5 mm, and three separate measurements are taken.

Despite the efforts of the writers of ASTM D1322 to clearly define the smoke point, there is still a level of subjectivity in the measurement; which is reflected in the ±3 mm reproducibility estimate quoted in the standard. This level of error is acceptable for low-to-medium sooting propensity fuels such as isooctane, but is a severe problem for fuels such as toluene which typically has a smoke point of around 6 mm. Reduction or elimination of the subjective elements of the test would therefore be a welcome development.

A characteristic of the smoke point which is used by some authors [9], is the presence of 'sooting wings'. These appear as a weakly luminescent region near the top of the flame with clearly defined sides, but no clear upper boundary, as illustrated in Fig. 1b. Unfortunately sooting wings are not usually observable for fuels with a high sooting propensity, and are therefore unsuitable as a universal criterion for the smoke point.

The **purpose of this paper** is to present the findings of an in-depth investigation into the smoke point test and explore how its accuracy, reproducibility and range of applicability can be enhanced. More specifically, the objectives are to:

- Investigate the relationship between fuel uptake rate and flame height, it has been suggested [10] that this may deviate from linear at the smoke point.
- Use this information to develop a more precise and objective measure of sooting tendency, whilst retaining as much of the simplicity of the standard test as possible.
- Prove the suitability of the proposed methodology to calculate the TSI for pure and blended fuels, reducing the error in the subjectivity of the measurements.

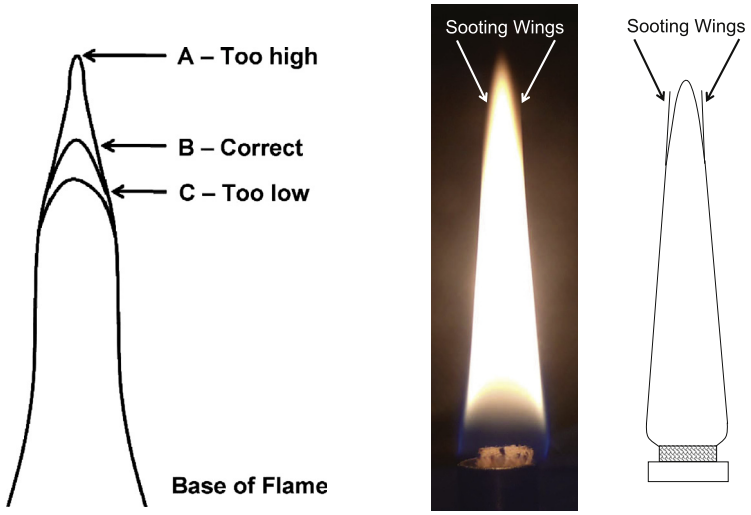

(a) Determination of the Smoke Point according to ASTM D1322

(b) Sooting wings for an iso-octane flame at its smoke point

Fig. 1. Definition of the smoke point.

2. Characterization of sooting propensity

2.1. Calculating the threshold sooting index

In practice, many of the experimental setups described in the literature to measure the sooting propensity of fuels do not conform to the design specified in ASTM D1322. The main reasons for this are that:

- The lamp is designed for aviation fuels and is unsuited to gaseous fuels, low-sooting fuels such as *n*-heptane or very strongly sooting fuels such as naphthalene.
- The boundary condition cannot be easily defined, which makes it difficult to model.

The smoke point is known to be a function of the apparatus design [11], meaning that some form of common standard is needed for smoke point measurements to be meaningful. It was suggested [12] that any such standard could have a simple inverse proportional relationship with the smoke point (h), measured in mm, however it was noted that this approach failed to account for the effect of stoichiometric ratio on flame height [13]. In order to solve this problem a 'Threshold Sooting Index' (TSI) was proposed [13], in which '0' = 'least sooting' and '100' = 'most sooting'. Assuming that the stoichiometric ratio was linearly related to the fuels' molecular weight (M_W), as well as allowing for some level of linear offset, this assumption lead to Eq. (1):

$$\mathrm{TSI} = a_h\left(\frac{M_W}{h}\right) + b_h \tag{1}$$

where a_h and b_h are apparatus-dependent constants if the smoke point is used.

Some authors [14,15] based their sooting propensity measurements on the 'critical equivalence ratio' (ϕ_e) at which soot was first produced in a premixed flame. It was also advocated that TSI could be defined in terms of the volumetric flow rate of fuel. The basis for this relation was the theory which predicted a proportional relationship between fuel volumetric flow ($\dot{V}$) rate and flame height [16].

In order to use all of these methods, arbitrary TSI values must be assigned to two reference fuels (indicated by subscripts 1 and 2) which can then be burned in the apparatus of interest. It is then possible to determine the apparatus-dependent constants a and b

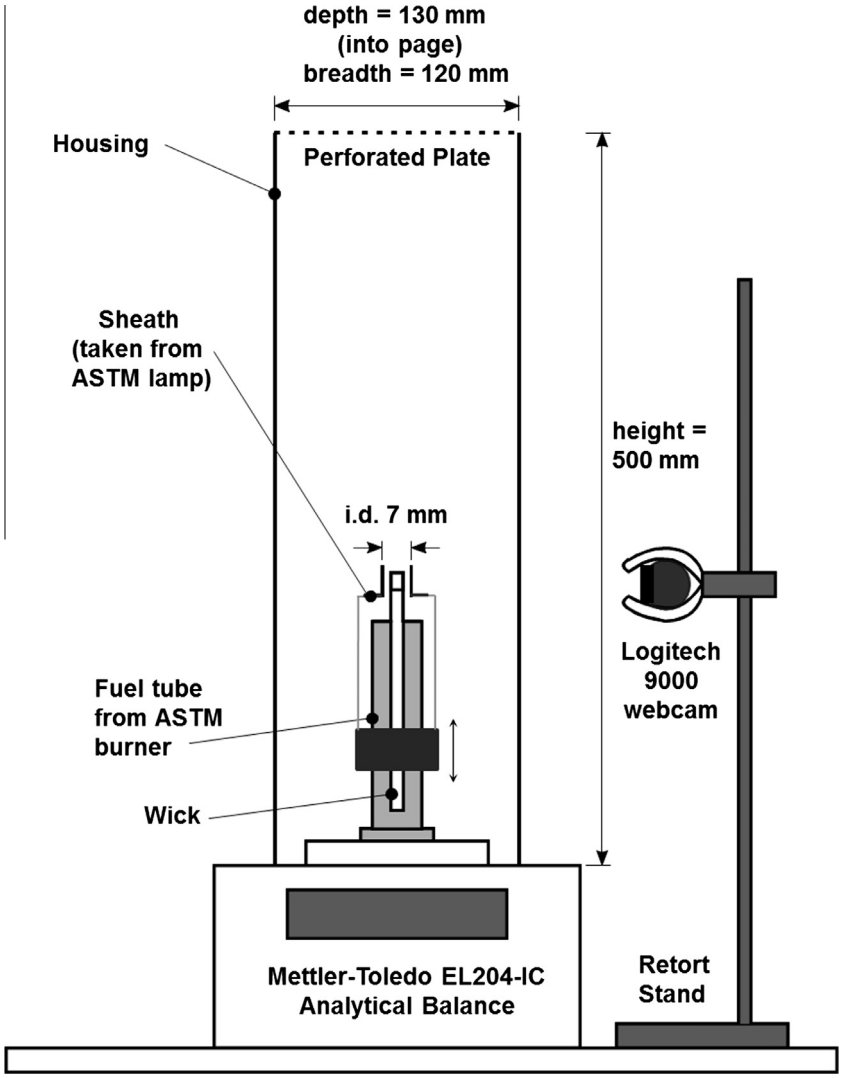

Fig. 2. Apparatus for determining flame height as a function of fuel uptake rate in a wick-fed burner.

by simultaneous solution. For the smoke point method this would yield Eqs. (2) and (3):

$$a_h = \frac{\mathrm{TSI}_1 - \mathrm{TSI}_2}{\left(\frac{M_{W1}}{h_1}\right) - \left(\frac{M_{W2}}{h_2}\right)} \tag{2}$$

$$b_h = \frac{\mathrm{TSI}_1\left(\frac{M_{W2}}{h_2}\right) - \mathrm{TSI}_2\left(\frac{M_{W1}}{h_1}\right)}{\frac{M_{W2}}{h_2} - \frac{M_{W1}}{h_1}} \tag{3}$$

It is also possible to determine a and b more precisely by least-squares fitting of smoke point data plotted against literature TSI values [10], however this approach is best avoided as it inevitably adds a certain amount of circularity to the analysis and consequently reduces the scientific validity of the results.

2.2. Strengths and weaknesses of the TSI metric

The TSI is useful because it has been found [17] to blend linearly with mole fraction in co-flow diffusion flames, as described by the following equation:

$$\mathrm{TSI}_{\mathrm{blend}} = \sum x_f \mathrm{TSI}_{\mathrm{Pure}} \tag{4}$$

The TSI is also of interest because it has been shown to be a good predictor of the amount of soot produced by real engines [18]. In its current form, the methodology for determining TSI nevertheless has a number of shortcomings:

1. The correlations for TSI are empirical in nature and the coefficients a and b have no basis in theory other than the inclusion of the M_W term in some of its forms. Even if the metric works well as a predictive tool in selected cases, its fundamental basis is still not understood, meaning that results cannot be extrapolated with confidence.
2. There is no widely recognized standard list of TSI values, meaning that the author has to assign reasonable values to a reference fuel based on what has already been reported in the literature. For example, Calcote and Manos [13] suggested TSI = 2 for n-hexane and TSI = 100 for 1-methyl naphthalene, whereas Mensch et al. [19] suggested using methylcyclohexane with TSI = 5 as the lower bound. Although Olson et al. [10] suggested some TSI reference values for a wide range of fuels, the uncertainties in these values are still unacceptably high; a further reason why better experimental methods are needed.

Recently, Li et al. [20] exposed a flaw in the definition of the TSI. The use of molecular weight is problematic for fuels that exhibit similar smoke points but have very different M_W. Therefore, when calculating the TSI, a higher sooting propensity will be attributed to the heavier fuel, even if they exhibit nearly same flame lengths at matched fuel mass flow rates [20]. This is the case of large n-alkanes, such as n-nonane and n-hexadecane. Due to this and the mentioned drawbacks, they suggest the normalization of the smoke point instead of the use of the TSI [20]. The weighted average of all the smoke point lengths reported in the literature for a certain fuel was proposed. Despite the absence of the mentioned TSI shortcomings, their results retains the extremely large errors in the smoke point, particularly for less sooting fuels. Errors as high as ±153 mm for propane are presented, or ±27 mm for n-nonane. This strengthens the need to find a less subjective measure with better reproducibility.

2.3. Other approaches

A proposal to improve the repeatability of sooting tendency measurements was recently made [21], suggesting the 'Yield Sooting Index' (YSI) as an alternative to the TSI. In the YSI test, laser incandescence is used to measure the maximum soot volume fraction, $f_{v,max}$ in a coflow methane/air non-premixed flame in which the fuel is doped with the test hydrocarbon. The quoted uncertainty of YSI values was 3%, provided that the correct amount of dopant is added to the flame; a significant improvement over that for the TSI. Following a further publication [22], YSI data are now available for a wide range of fuels.

Another alternative standard, named the Micropyrolysis Index (MPI) was developed [23]. The main objective of this approach was to obtain a result that was independent of operating conditions such as temperature and oxygen supply. The test fuel is pyrolysed, and the amount of deposited carbon was then quantified to measure the sooting tendency of the fuel. The correlation between TSI and MPI was not as strong at that with YSI, although the data set used is much more limited [23].

The main disadvantage of the YSI and MPI approaches is that they require a greater level of investment than the smoke point method; both in terms of the cost of the equipment and in the technical knowledge and experience needed to use them.

2.4. Adapted smoke point test

Earlier work [10] suggested that the smoke point method could be modified by measuring the fuel uptake rate at the smoke point, rather than the smoke point itself; indeed this approach was used in previously by Schalla and Macdonald [24]. Thus, the TSI would be given by:

$$\mathrm{TSI} = a_m\left(\frac{M_W}{\dot{m}}\right) + b_m \tag{5}$$

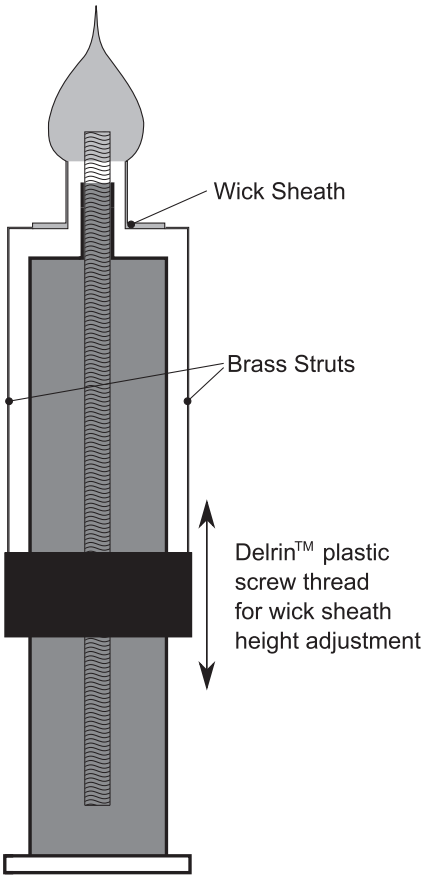

Fig. 3. The modified light-weight burner.

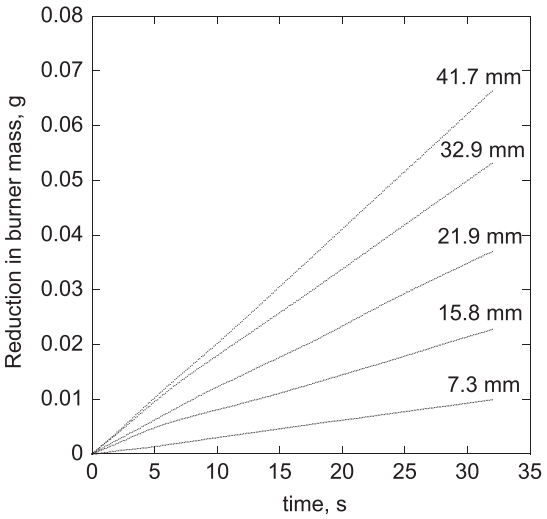

Fig. 4. Mass of fuel consumed vs time for a range of flame heights.

The basis for this suggestion was an observation reported by Jezl [25] that when experimental measurements of flame height were plotted against fuel uptake rate, the smoke point occurred at a distortion in the resulting curve. There were thought to be two main advantages of using the fuel uptake rate as opposed to the flame height; firstly it could be measured more precisely and secondly the shape of the distortion was thought to be such that the fuel uptake rate would not be very sensitive to the flame height in the region around the smoke point. It was claimed that the uncertainty of the method was ±7% [19], although others [10] implied that this was merely the readability of the uptake rate measurement, without accounting for other factors such as human error. Olson et al. [10] included some plots of fuel uptake rate vs flame height in their work, in which a distortion could be observed around the smoke point. Unfortunately there were insufficient data to show the shape of the distortion, or even to show conclusively that it existed. Further verification is therefore required before it can be conclusively stated that the fuel uptake rate method is better than the smoke point method for determining TSI.

Table 1
Toluene reference fuel blends used in the flame height vs fuel uptake rate tests.

Blend no.	Toluene (% vol.)	Isooctane (% vol.)	N-heptane (% vol.)	Smoke point (mm)	Absolute error (±, 95% confidence)
1	100	0	0	7.3	1.2
2	66.7	16.67	16.67	10.8	1.3
3	50	50	0	8.9	0.9
4	50	0	50	13.7	1.4
5	33.3	33.3	33.3	16.5	3.1
6	16.67	66.7	16.67	21.7	2.6
7	16.67	16.67	66.7	25.7	7.4
8	0	100	0	38.7	1.4
9	0	50	50	53.2	7.0
10	0	0	100	72	18

3. Experimental methods

An improved methodology and laboratory setup Fig. 2 were developed in order to confirm previous findings [10], of a distortion in the plots of fuel uptake rate vs flame height. Complete explanation of the experimental set-up and the image analysis is given, followed by the description on how the new proposed methodology was tested.

3.1. Set-up and methodology

The smoke point lamp burner was redesigned so that its weight, including the flame adjustment mechanism, was less than the maximum allowed by the balance. The burner was adapted by fitting a Delrin™ thread to the outside of the burner tube and connecting this to the wick sheath via four brass struts, as depicted in Fig. 3. Thus, the flame height could be adjusted by rotating the threaded fitting, i.e. fuel uptake rate could be modified. Use of a Delrin™ fitting was required, as a brass thread would have increased the weight beyond the maximum weight allowed by the balance.

It was decided that the approach of simply weighing the burner before and after each trial in order to determine the fuel uptake rate was unsatisfactory, since it failed to take into account evaporation of the fuel either during the lighting of the flame or as the

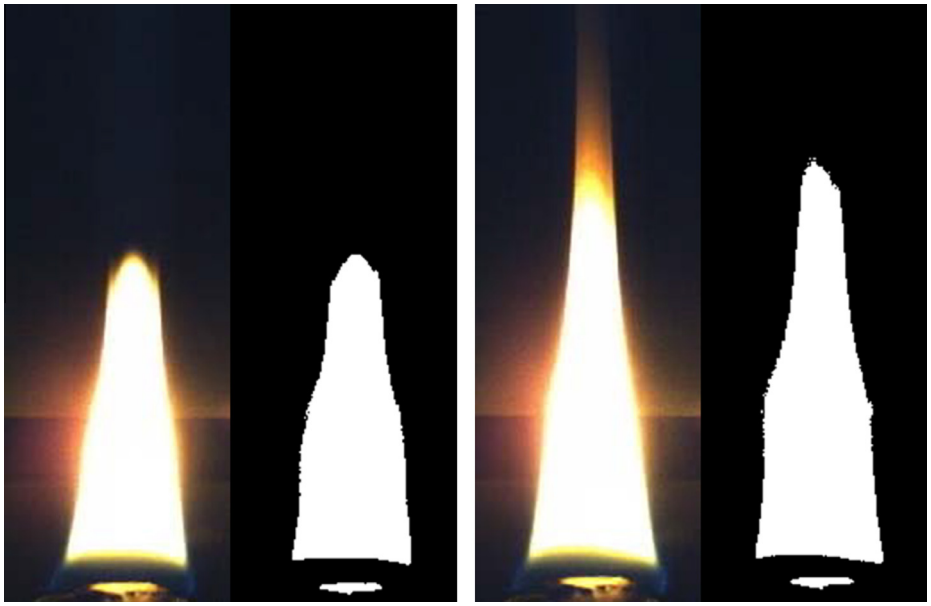

Fig. 5. Image analysis for two isoctane flame: 41 mm flame height (left) and 60 mm flame height (right).

burner was being transferred to the balance. This problem was solved by continuous weighing of the burner followed by linear regression of the resulting values in order to determine the fuel uptake rate. The gradient of the least-squares regression line was then used to determine the fuel uptake rate, after rejection of any data that clearly deviated from linear. Excellent linearity was nevertheless obtained in the majority of cases. Typical raw data obtained from this approach are shown in Fig. 4, although individual data points are not distinguishable due to the high frequency of sampling.

For each flame height, the mass of the burner and its contents was logged for a minimum of 1 min using LabX direct software and a Mettler-Toledo EL204-IC analytical balance of readability 0.1 mg. The flame height itself was measured with the aid of a Logitech 9000 Webcam, which was used in 1280×720 mode at 20 frames per second. The camera was positioned so that a resolution better than 0.2 mm could be obtained. Footage was recorded over approximately the same duration as the mass measurements.

3.2. Image analysis

The videos of the flame experiments were imported to MATLAB. A script was written to quantify the flame height of each frame (image), allowing calculation of the mean flame height as well as the statistical uncertainty in the value. Each image was converted to greyscale and cropped at the base of the flame, then converted to binary format by application of a light intensity threshold. This threshold was chosen to best describe the shape of the flame, and represents the minimum light intensity necessary to be considered as a flame point. Above this threshold the pixel would be white and below the threshold the pixel would be black. Hence, the flame could be mapped as all white pixels in the image, an example of this analysis is presented in Fig. 5. The script was then used to map the highest row to contain a white pixel, which corresponds to a height after which the intensity is less than the defined threshold.

A calibration rod of length 100 mm was inserted into the wick sheath and photographed. The image could then be imported to MATLAB and cropped to obtain the number of pixels, N_p, occupied by the rod. The number of pixels per real-life millimeter was therefore given by N_p divided by 100 mm.

This technique accounted for fluctuations in the flame height and established an objective measure of the tip position. The latter is particularly difficult to do by eye, because once the flame is above its smoke point the upper boundary of the flame ceases to be well-defined. The use of light intensity (related to flame temperature and soot concentration) as reference to measure the height of the flame, instead of the shape of the tip of the flame, is suggested as a less subjective definition for posterior calculations of sooting propensity.

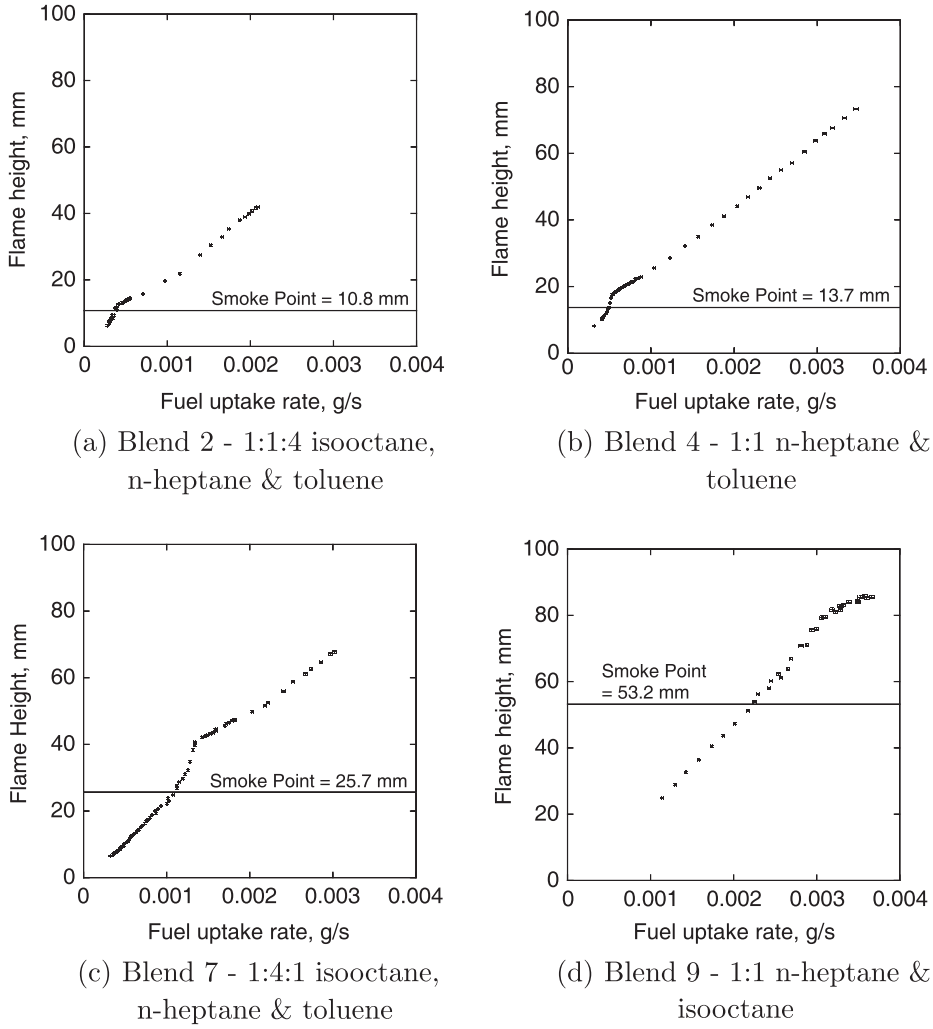

(a) Blend 2 - 1:1:4 isooctane, n-heptane & toluene

(b) Blend 4 - 1:1 n-heptane & toluene

(c) Blend 7 - 1:4:1 isooctane, n-heptane & toluene

(d) Blend 9 - 1:1 n-heptane & isooctane

Fig. 6. Flame height vs fuel uptake rate curves for 10 toluene reference fuel blends.

3.3. Testing the new methodology

The findings from the experiments described in Section 3.1 indicated that there was potential to improve the reproducibility of the smoke point test by making certain alterations to the equipment and procedure used. In order to determine whether or not the current smoke point test should be adapted, three methodologies were compared:

1. The 'traditional' ASTM method, in which the flame wick sheath was adjusted until the flame morphology corresponded with point B in Fig. 1a. The flame height was then measured using two rulers in front and behind in order to eliminate parallax error. Flame height was defined as the distance between the upper edge of the wick sheath and the tip of the flame.
2. The method of Olson et al. [10] (O&P), which was identical to method 1, except that the fuel uptake rate was measured instead of the flame height.
3. A new method: fuel uptake rate measurement with threshold imaging (FURTI). Where the flame was adjusted and the fuel uptake was measured at each height. The fuel uptake rate at the point when the flame showed maximum sensitivity to mass flow rate was chosen to calculate the TSI.

To test the reproducibility of the new methodology, each procedure (each fuel tested) was carried out nine times by at least two different experimentalists.

4. Results and discussion

4.1. Relationship between flame height and fuel uptake rate

In order to confirm the findings of Olson et al. [10] over a wide range of smoke points, a set of 10 toluene reference fuels was used, as outlined in Table 1. The smoke points were determined using the ASTM D1322 criterion, applied to the setup in Fig. 2. Percentages are given in terms of volume fraction of the component fuel.

Four of the flame height vs fuel uptake rate curves are displayed in Fig. 6, together with the ASTM smoke point estimates as indicated by the thick horizontal line. There is some scatter in the data which falls outside the error bounds, and this is thought to be due mainly to interference between the sheath which is used to control the flame height and the cotton 'burr' at the top of the wick. The tendency of strongly sooting flames to fill the burner housing with large soot agglomerates is also a potential source of error.

Despite the limitations of the data, it was observed that the distortion mentioned before [10] was present in almost all cases, with the exception of pure n-heptane, where the general trend suggests that any distortion would occur outside the range of the apparatus. For most of the blends, the data initially show a linear relationship between flame height and fuel uptake rate, before tending towards a vertical asymptote, then deviating sharply back to near-linearity. It is important to note that the smoke point seems to occur at the first linear region of the curve, before the inflexion. This contradicts previous findings [10] and implies that basing the TSI on the fuel uptake rate at the smoke point is unlikely to yield much improvement in reproducibility such that because the smoke point occurs in the linear region of the curve, the uptake rate and resulting TSI value will be subject to approximately the same level of human error as before.

This inflexion point after which the flame seems to be less sensitive to increments in the mass flow rate is related to our definition of the flame height. After the smoke point, once the tip of the flame ceases to be well defined, and regularly a soot trail appears, the light intensity decreases because the temperature of the soot particles (being out of the flame) decreases. The flame height measurement obtained through the proposed image analysis allows to distinguish this stage, before which high concentration of soot particles are still contained inside the flame, and after which the visual flame grows more slowly due to higher concentration of soot passing through it.

By examining the video footage more closely, it was possible to identify certain flame morphologies with particular regions of the flame height – mass uptake curve, as illustrated in Fig. 7. In order

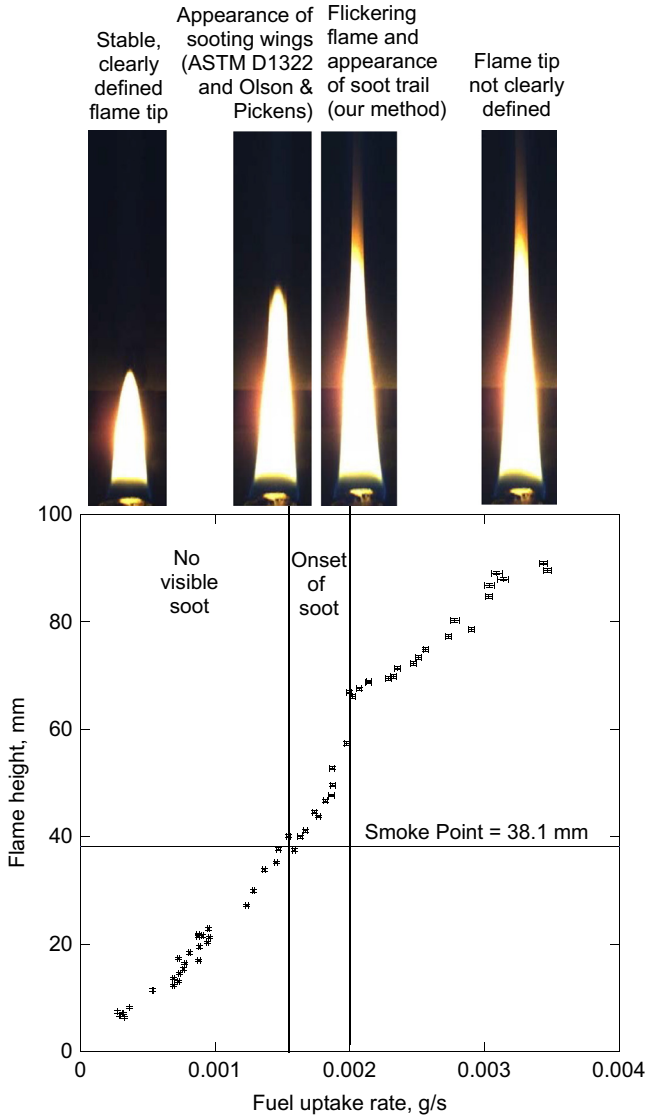

Fig. 7. Flame morphologies at important points on the flame height vs fuel uptake rate curve for blend 8.

Table 2
Coefficients in the TSI equation and associated errors for methods 1, 2 and 3.

ASTM	a	σ_a (±)	Units	b	σ_b (±)
Traditional	4.03	0.75	mol g^{-1} mm^{-1}	−8.24	2.61
O&P	1.06×10^{-4}	7×10^{-6}	mol s^{-1}	−2.67	1.29
FURTI (this work)	1.18×10^{-4}	4×10^{-6}	mol s^{-1}	−1.12	0.25

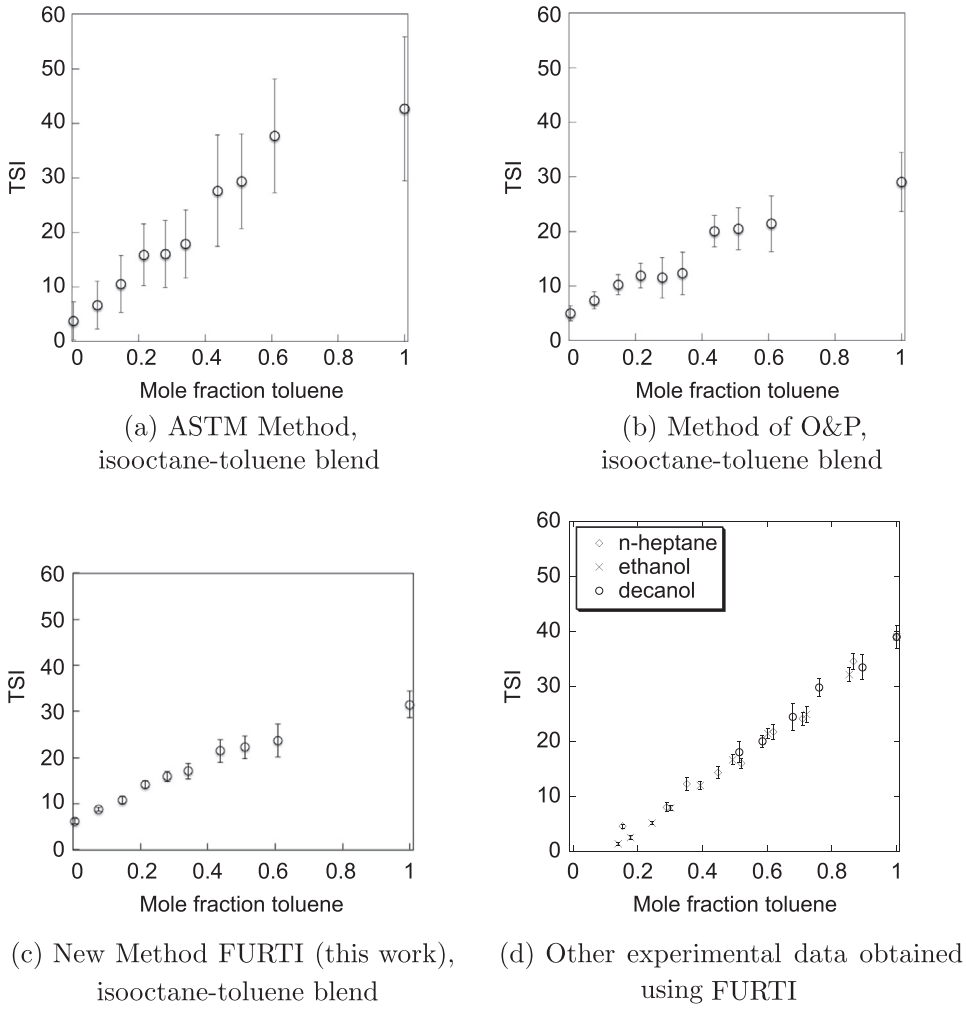

(a) ASTM Method, isooctane-toluene blend

(b) Method of O&P, isooctane-toluene blend

(c) New Method FURTI (this work), isooctane-toluene blend

(d) Other experimental data obtained using FURTI

Fig. 8. TSIs, based on a variety of methods, for a variety of component fuels blended with toluene.

to minimize the sensitivity to human error, it can be surmised that the best point to measure fuel uptake rate is when the flame height is most sensitive to wick adjustment, i.e. the point of the steepest gradient in Fig. 7.

4.2. Comparing methodologies

It was found that the percentage error in the raw values, i.e. smoke point and fuel uptake rate, were approximately halved by using the new method FURTI instead of the ASTM standard; however to gain a true estimate of the extent to which the new method is better, it is necessary to convert the raw measurements to TSI values, together with the associated error estimates.

Table 3
TSI values and associated error bounds for the ASTM, O&P and FURTI.

Fuel	TSI, ASTM			TSI, O&P			TSI, FURTI		
		Error			Error			Error	
		±	%		±	%		±	%
1-Methylnaphthalene	100.0	8.4	**8.42**	100.0	2.8	**2.8**	100.0	1.2	**1.2**
50% n-heptane, 50% tol.	26.5	7.7	**28.9**	18.9	3.4	**17.9**	21.7	1.4	**6.5**
66% n-heptane, 34% tol.	18.1	6.1	**33.9**	12.4	2.4	**19.6**	14.3	1.0	**7.3**
75% n-heptane, 25% tol.	14.3	5.7	**39.5**	10.8	2.0	**18.6**	12.2	1.2	**9.4**
Phenylcyclohexane	107.9	22.7	**21.0**	66.3	4.8	**7.3**	69.1	2.3	**3.4**
Methylcyclohexane	5.0	4.9	**97.3**	5.0	1.4	**27.9**	5.0	0.3	**5.6**

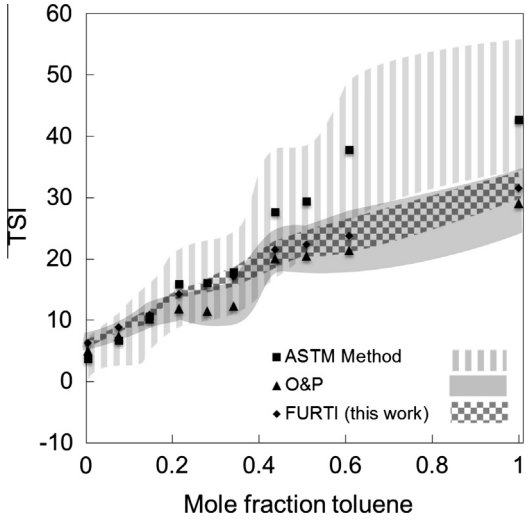

Fig. 9. Comparison of results for blends of iso-octane and toluene for each method.

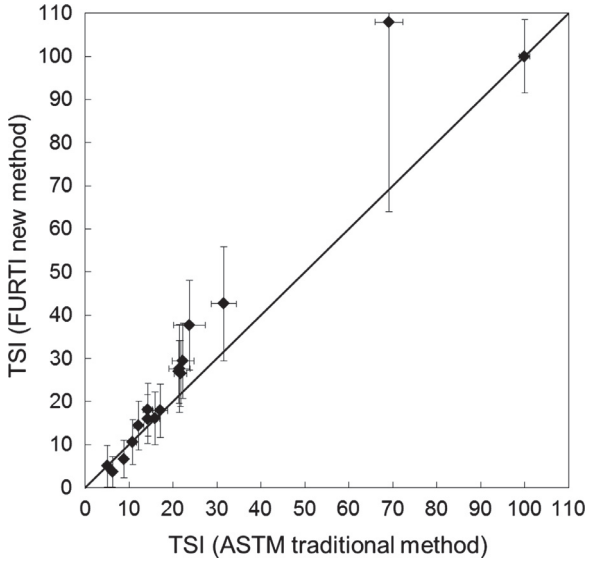

(a) TSI correlation between traditional method and new method FURTI

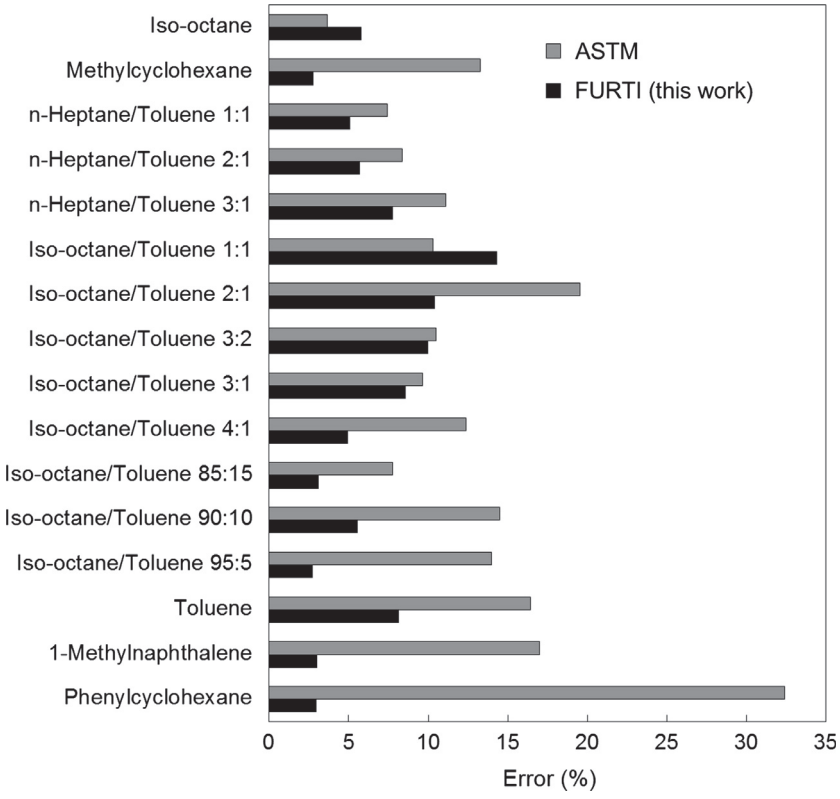

(b) Comparison of experimental errors in raw results from the ASTM and FURTI

Fig. 10. TSI comparison between traditional method and new method FURTI.

Assuming that the TSI values for 1-methylnaphthalene and methylcyclohexane are 100 and 5 respectively, it was possible to calculate values for the coefficients a and b for each of the methods using Eqs. (2) and (3). Using the standard methodology, error propagation equations were then used to derive the following equations in order to gain an estimate of the overall errors, σ_a and σ_b, in the two coefficients:

$$\sigma_a = a\sqrt{\frac{\left(\frac{M_{W1}}{h_1^2}\sigma_{h1}\right)^2+\left(\frac{M_{W2}}{h_2^2}\sigma_{h2}\right)^2}{\left(\left(\frac{M_{W1}}{h_1}\right)-\left(\frac{M_{W2}}{h_2}\right)\right)^2}} \tag{6}$$

$$\sigma_b = b\sqrt{\frac{\left(TSI_2\left(\frac{\sigma_{h1}M_{W1}}{h_1^2}\right)\right)^2+\left(TSI_1\left(\frac{\sigma_{h2}M_{W2}}{h_2^2}\right)\right)^2}{\left(TSI_2\left(\frac{M_{W1}}{h_1}\right)-TSI_1\left(\frac{M_{W2}}{h_2}\right)\right)^2}+\frac{\left(\frac{M_{W1}}{h_1^2}\sigma_{h1}\right)^2+\left(\frac{M_{W2}}{h_2^2}\sigma_{h2}\right)^2}{\left(\left(\frac{M_{W1}}{h_1}\right)-\left(\frac{M_{W2}}{h_2}\right)\right)^2}} \tag{7}$$

Table 4
Smoke points and critical fuel uptake rates for the ASTM, Olson & Pickens (O&P) and new methods.

Fuel	ASTM, smoke point (mm)			O& P, Fuel uptake rate (μg/s)			FURTI, Fuel uptake rate (μg/s)		
		Error			Error			Error	
		±	%		±	%		±	%
1-Methylnaphthalene	5.3	0.9	**17.0**	147	9	**6.1**	166	5	**3.0**
Phenylcyclohexane	5.6	1.8	**32.8**	246	15	**6.1**	269	8	**3.0**
Toluene	7.3	1.2	**16.4**	308	47	**15.2**	333	27	**8.1**
50% n-heptane, 50% tol.	11.1	0.8	**7.4**	471	60	**12.8**	494	25	**5.1**
50% isooctane, 50% tol.	8.9	0.9	**10.3**	448	87	**19.4**	484	69	**14.3**
60% isooctane, 40% tol.	11.2	1.2	**10.5**	477	68	**14.2**	525	52	**10.0**
66% n-heptane, 33% tol.	14.9	1.2	**8.4**	684	82	**11.9**	742	42	**5.7**
66% isooctane, 33% tol.	11.9	2.3	**19.6**	493	44	**9.0**	552	57	**10.4**
75% n-heptane, 25% tol.	17.5	1.9	**11.1**	769	71	**9.2**	865	67	**7.8**
75% isooctane, 25% tol.	16.7	1.6	**9.6**	762	182	**23.8**	696	60	**8.6**
80% isooctane, 20% tol.	18.1	2.2	**12.4**	814	194	**23.9**	753	37	**4.9**
85% isooctane, 15% tol.	18.4	1.4	**7.7**	801	90	**11.2**	847	26	**3.1**
90% isooctane, 10% tol.	24.0	3.5	**14.5**	917	71	**7.8**	1098	61	**5.5**
95% isooctane, 5% tol.	30.7	4.3	**14.0**	1191	65	**5.5**	1335	36	**2.7**
Iso-octane	38.7	1.4	**3.7**	1582	74	**4.7**	1832	106	**5.8**
Methylcyclohexane	30.1	4.0	**13.4**	1360	207	**15.3**	1894	52	**2.7**

Table 5
TSI values and associated error bounds for the ASTM, O& P and FURTI.

Fuel	TSI, ASTM			TSI, O& P			TSI, FURTI		
		Error			Error			Error	
		±	%		±	%		±	%
Toluene	42.7	13.2	**30.9**	29.1	5.4	**18.7**	31.5	2.9	**9.1**
50% isooctane, 50% tol.	37.7	10.4	**27.6**	21.4	5.1	**23.8**	23.7	3.7	**15.4**
60% isooctane, 40% tol.	29.4	8.7	**29.6**	20.5	3.8	**18.8**	22.3	2.5	**11.1**
66% isooctane, 33% tol.	27.6	10.2	**36.9**	20.0	2.9	**14.3**	21.5	2.5	**11.5**
75% isooctane, 25% tol.	17.9	6.2	**34.8**	12.3	9.9	**31.9**	17.1	1.7	**9.9**
80% isooctane, 20% tol.	16.1	6.2	**38.4**	11.5	3.7	**32.5**	15.9	1.0	**6.5**
85% isooctane, 15% tol.	15.9	5.7	**35.6**	11.9	2.3	**19.3**	14.2	0.7	**5.2**
90% isooctane, 10% tol.	10.5	5.2	**49.6**	10.2	1.8	**18.0**	10.8	0.8	**7.5**
95% isooctane, 5% tol.	6.7	4.4	**66.1**	7.4	1.6	**21.0**	8.8	0.5	**5.5**
Iso-octane	3.7	3.5	**94**	5.0	1.4	**28.7**	6.2	0.6	**8.8**

Where necessary, the fuel uptake rate and its error bounds could be substituted for the smoke point of the reference fuels, h_1 and h_2 and the associated errors, σ_{h1} and σ_{h2}. The results of the TSI calculations are summarized in Table 2. Note that coefficient b is always dimensionless.

The error in TSI is then given by Eqs. (2) and (3)

$$\sigma_{TSI} = \sqrt{a^2\left(\frac{M_W}{h}\right)^2\left(\left(\frac{\sigma_a}{a}\right)^2+\left(\frac{\sigma_h}{h}\right)^2\right)+\sigma_b^2} \quad (8)$$

The final TSI values and error bounds are shown in Fig. 8 for blends and Table 3 for pure components. Using FURTI, blends of toluene and isocetane, ethanol, n-heptane and decanol were also investigated (see Fig. 8d).

In order to compare the results from each method, the isooctane-toluene data are plotted together on Fig. 9, together with the loci of the error estimates for each data set:

Table 6
Basic rules of error propagation for a function, f, where σf is the uncertainty associated with the value of the function f.

Function	Standard error	
1	$f = A \pm B$	$\sigma_f = \sqrt{\sigma_A^2+\sigma_B^2}$
2	$f = xA^{\pm y}$	$\sigma_f = yf\frac{\sigma_A}{A}$
3	$f = AB,\ f = \frac{A}{B}$	$\sigma_f = f\sqrt{\left(\frac{\sigma_A}{A}\right)^2+\left(\frac{\sigma_B}{B}\right)^2}$

It can be seen from Table 3 and Fig. 8 that the errors in the TSI values for the ASTM method were generally much higher than the value of 15% quoted in the literature [21], to the extent that the lower TSI values are essentially meaningless. Presumably this is because the error in the calibration procedure itself is rarely taken into account; which might explain the wide variation in the literature TSI values. Fig. 10a is also of interest because it shows that the two methods based on fuel uptake rate give consistent results, despite the difference in the way the measurement is taken. By contrast, the results from the ASTM method appeared to be inconsistent with both of the other methods.

Fig. 10 presents a comparison of TSI values calculated using the traditional method and the new method FURTI. According to Fig. 10a the new method consistently presents TSI values larger than the traditional method, although the large errors in the traditional method do not allow to draw specific conclusions.

5. Conclusions

A new method for determining the TSI is been proposed in which the fuel uptake rate is measured at the point when the flame height exhibits maximum sensitivity to changes in mass flow rate. The method has been shown to yield results which are typically subject to less than half the statistical uncertainty of other previously reported methods using similar apparatus. The new method introduces a less subjective definition to calculate the TSI using image analysis and a light intensity threshold, and delivers improved results in the majority of cases, particularly for aromatics, and the fuel blends for which it is unsuited are easily identifiable from the flame morphology.

Acknowledgements

We gratefully acknowledge the contributions of Mr. Rui Hui and Mr. Chin Kiat Tan, who assisted with the experimental work described in this paper as part of their respective degree courses; the invaluable feedback from our colleagues Dr. Andrew Smallbone, Dr. Sebastian Mosbach and Dr. Jethro Akroyd; the financial support of the EPSRC under the Grant EP/I01165X/1.

Appendix A

A.1. Smoke Point Results

Tables 4 and 5.

A.1.1. Error analysis

In order to estimate how errors in smoke point translate through to errors in TSI, Taylor expansions of generic functions are used to derive the simple rules shown in Table 6:

The reference fuels, namely 1-methylnaphthalene and methylcyclohexane, are used to calibrate the apparatus (i.e. to find a and b). Referring to these fuels using subscripts 1 and 2 respectively, their TSI values are given by Eqs. (9) and (10):

$$TSI_1 = a\left(\frac{M_W}{h_1}\right) + b \tag{9}$$

$$TSI_1 = a\left(\frac{M_W}{h_2}\right) + b \tag{10}$$

where M_W and h are the molecular weights and smoke points respectively of fuels 1 and 2. Hence by simultaneous solution:

$$a = \frac{TSI_1 - TSI_2}{\left(\frac{M_W}{h_1}\right) - \left(\frac{M_W}{h_2}\right)} \tag{11}$$

$$b = \frac{TSI_2\left(\frac{M_W}{h_1}\right) - TSI_1\left(\frac{M_W}{h_2}\right)}{\left(\frac{M_W}{h_1}\right) - \left(\frac{M_W}{h_2}\right)} \tag{12}$$

Using a special case of rule 3 in Table 6, the 95% confidence interval in a function of the form $f = k/A$ is given by:

$$\sigma_f = k\sigma_A/A^2 \tag{13}$$

Applying rules 1 and 3 from Table 6 as well as Eq. (13), yields Eqs. (6) and (7):

Note that the reference TSIs are defined values and hence have no associated experimental error.

References

[1] Pope CA, Dockery DW. Health effects of fine particulate air pollution: lines that connect. J Air Waste Manage Assoc 2006;56:709–42.

[2] Seaton A, Godden D, MacNee W, Donaldson K. Particulate air pollution and acute health effects. The Lancet 1995;345(8943):176–8.

[3] Balthasar M, Frenklach M. Monte-carlo simulation of soot particle coagulation and aggregation: the effect of a realistic size distribution. Proc Combust Inst 2005;30(1):1467–75. http://dx.doi.org/10.1016/j.proci.2004.07.035.

[4] Singh J, Patterson RI, Kraft M, Wang H. Numerical simulation and sensitivity analysis of detailed soot particle size distribution in laminar premixed ethylene flames. Combust Flame 2006;145(1G2):117–27. http://dx.doi.org/10.1016/j.combustflame.2005.11.003.

[5] Celnik MS, Sander M, Raj A, West RH, Kraft M. Modelling soot formation in a premixed flame using an aromatic-site soot model and an improved oxidation rate. Proc Combust Inst 2009;32(1):639–46. http://dx.doi.org/10.1016/j.proci.2008.06.062.

[6] Echavarria CA, Sarofim AF, Lighty JS, DAnna A. Modeling and measurements of size distributions in premixed ethylene and benzene flames. Proc Combust Inst 2009;32(1):705–11. http://dx.doi.org/10.1016/j.proci.2008.06.172.

[7] Echavarria CA, Sarofim AF, Lighty JS, DAnna A. Evolution of soot size distribution in premixed ethylene/air and ethylene/benzene/air flames: experimental and modeling study. Combust Flame 2011;158(1):98–104. http://dx.doi.org/10.1016/j.combustflame.2010.07.021.

[8] Chen D, Zainuddin Z, Yapp E, Akroyd J, Mosbach S, Kraft M. A fully coupled simulation of pah and soot growth with a population balance model. Proc Combust Inst 2013;34(1):1827–35. http://dx.doi.org/10.1016/j.proci.2012.06.089.

[9] Glassman I, Yaccarino P. The temperature effect in sooting diffusion flames. In: Eighteenth Symposium (International) on Combustion; 1981. p. 1175–83.

[10] Olson D, Pickens J, Gill R. The effects of molecular structure on soot formation II. diffusion flames. Combust Flame 1985;62(1):43–60.

[11] Rakowsky FW, Hunt RA. Variables in lamp design that affect smoke point. Anal Chem 1956;28(10):1583–6. http://dx.doi.org/10.1021/ac60118a024.

[12] Minchin S. Luminous stationary flames: the quantitative relationship between flame dimension at the sooting point and chemical composition. J Inst Petrol Technol 1931;17:102–20.

[13] Calcote HF, Manos DM. Effect of molecular structure on incipient soot formation. Combust Flame 1983;49(1–3):289–304.

[14] Street JC, Thomas A. Carbon formation in premixed flames. Fuel 1955;34(4):4–36.

[15] Blazowski WS. Dependence of soot production on fuel structure in backmixed combustion. Combust Sci Technol 1980;21(3-4):87–96. http://dx.doi.org/10.1080/00102208008946922.

[16] Burke SP, Schumann TEW. Diffusion flames. Indust Eng Chem 1928;20(10):1–7. http://dx.doi.org/10.1021/ie50226a005.

[17] Gill R, Olson D. Estimation of soot thresholds for fuel mixtures. Combust Sci Technol 1984;40(5):307–15.

[18] Yang Y, Boehman AL, Santoro RJ. A study of jet fuel sooting tendency using the threshold sooting index (TSI) model. Combust Flame 1985;149(1–2):191–205.

[19] Mensch A, Santoro RJ, Litzinger TA, Lee SY. Sooting characteristics of surrogates for jet fuels. Combust Flame 2010;157:1097–105.

[20] Li L, Sunderland PB. An improved method of smoke point normalization. Combust Sci Technol 2012;184(6):829–41. http://dx.doi.org/10.1080/00102202.2012.670333.

[21] McEnally C, Pfefferle LD. Improved sooting tendency measurements for aromatic hydrocarbons and their implications for naphthalene formation pathways. Combust Flame 2007;148(4):210–22.

[22] McEnally C, Pfefferle LD. Sooting tendencies of oxygenated hydrocarbons in laboratory-scale flames. Environ Sci Technol 2011;45(6):2498–503.

[23] Crossley SP, Alvarez WE, Resasco DE. Novel micropyrolyis index (mpi) to estimate the sooting tendency of fuels. Energy Fuels 2008;22(4):2455–64.

[24] Schalla R, McDonald G. Variation in smoking tendency among hydrocarbons of low molecular weight. Indust Chem Chem 1953;45(7):1497–500.

[25] Jezl JL. Report no. d1016. Tech. Rep.; Sun Oil Co., Research and Development; 1950.